Conformational Transition of Polyelectrolytes in Mixed Solvent by Dielectric Spectroscopy: Electrostatic and Hydrophobic Interactions

Xinlu Zhou, Kongshuang Zhao

College of Chemistry, Beijing Normal University, Beijing 100875, China
Correspondence to: K. Zhao (E-mail: zhaoks@bnu.edu.cn)

Received 21 July 2019; revised 23 October 2019; accepted 28 October 2019; published online 27 November 2019
DOI: 10.1002/polb.24906

ABSTRACT: We studied conformational transition of poly(acrylic acid)-graft-dodecyl (PAA-g-dodecyl), and PAA-graft-poly(ethylene oxide)-graft-dodecyl (PAA-g-PEO-g-dodecyl) molecules in DMF/H_2O solvent by dielectric analysis method utilizing a double-layer polarization theory. In addition to the hydrophobic interaction which has been demonstrated to be vital for their conformational transition with water content, it is confirmed that the electrostatic interaction is crucial. For PAA-g-dodecyl molecules, at a critical value of water content, a peak value of correlation length is reached originating from the delicate balance between electrostatic and hydrophobic interactions. For PAA-g-PEO-g-dodecyl molecules, chains conformation is mainly determined by electrostatic interaction over the entire range of water content due to the low content of dodecyl groups. Meanwhile, H-bond associative interaction prevents the dissociation of free carboxyl groups over the range of lower water content, thus their stretched transition moves to higher water content. Our results provide the underlying insights needed to understand solvent effect on the conformational transition for polyelectrolytes with hydrophobic groups. © 2019 Wiley Periodicals, Inc. J. Polym. Sci., Part B: Polym. Phys. **2019**, *57*, 1716–1724

KEYWORDS: polyelectrolyte; chain conformation; interactions; mixed solvent; dielectric analysis

INTRODUCTION Polyelectrolytes containing some hydrophobic groups being part of the backbone in homopolymers or being grafted to the backbone form a very important class of polymers. In the past several years, chain conformation of this kind of polyelectrolyte has attracted considerable attentions, but has not yet gained a similar level of understanding as their neutral or hydrophilic counterparts due to the coexistence of electrostatic and hydrophobic interactions.[1,2] It is well known that one easily accessible way to control these interactions is to change solvent qualify.[2–4] Usually, when polyelectrolytes are dissolved in the good solvent, chains adopt stretched conformation.[2] When polyelectrolytes are dissolved in the poor solvent, an necklace model[3,4] was proposed to describe chain conformation, which was then confirmed by some simulation and experimental studies.[5,6] In the mixture of good and poor solvent, some researches showed that hydrophobic polyelectrolytes undergo an abrupt conformational transition from collapsed to extended structure when the ratio of good solvent increases to a certain ratio.

From the viewpoints of interactions, numerous studies showed that the solvent plays an important role by controlling monomers–solvent and monomers–monomers interaction.[7–11] On the one hand, when the solvent qualify is low, hydrophobic attractive interaction is high, causing the collapse.[7,13,14] On the other hand, few researches proposed that when the dielectric permittivity of the solvent is low, the effect of condensation of counterions onto chains is obvious, causing the decrease of electrostatic repulsive interaction between segments and the collapse of molecules.[12,15,16]

In order to clarify the effect of solvent qualify, it is necessary to explore how the electrostatic and hydrophobic interactions balance in the process of conformational transition. In view of the situation, several factors that influence electrostatic repulsion interaction between segments including the fraction of effective charges on chains, the distribution of counterions,[17,18] as well as the existence of hydrophilic associative groups which expand the application of polyelectrolytes as templates,[19] molecular actuators,[20] and drug carrier,[21] are worth further consideration.

In order to understand and answer above issues, a technique which can be used to capture microstructural and electrical information of polyelectrolyte is needed. The frequency-domain dielectric relaxation spectroscopic (DRS), owing to its sensibility to all kinds of polarization, can provide important, sometimes unique information on charge distribution, movements of molecules or ions, and intermolecular interactions.[22–27] In fact, the DRS method has been extensively applied to provide much valuable information including chains conformation,[22,23] the effective charges on chains,[24] the distribution of counterions around

Additional Supporting Information may be found in the online version of this article.

chains,[25,26] as well as various complex interactions.[27] In the previous works, we have obtained the correlation length, zeta potential, and linear density of counterions around chains of poly(acrylic acid) (PAA) and PAA-graft-poly(ethylene oxide)-graft-dodecyl (PAA-g-PEO-dodecyl) side chains in aqueous solution by analyzing dielectric spectroscopy based on the double-layer polarization model (DLPM).[28–30] Based on these parameters, we explained some fundamental issues about chain conformation of polyelectrolytes in aqueous solution.

In this study, a main goal is to explore the delicate balance of electrostatic and hydrophobic interactions in the process of conformational transition with water content for polyelectrolylte containing hydrophobic groups. The dielectric analysis on solution systems of PAA-g-dodecyl and PAA-g-PEO-g-dodecyl in *N,N*-Dimethylformamide (DMF)/H_2O mixed solvent was performed by the DLPM. The molecular structures are described in Scheme 1. For PAA-g-dodecyl molecules (the weight fraction of dodecyl side chains $\omega_{\text{dodecyl}} \approx 26\%$), H_2O is a poor solvent and DMF is a good solvent.[27] The results suggest that the change of electrostatic interaction with water content is important for their evolution of chains conformation. The balance of electrostatic and hydrophobic interactions of molecules in mixed solvent is influenced by H-bond associative interaction and the content of dodecyl groups. Besides, the influences of effective charges on their conformational transition were examined.

Double-Layer Polarization Model

The model follows relevant assumptions in scaling theory and Mandel theory about chains conformation of polyelectrolytes in solution. A polyelectrolyte chain adopts a random walk configuration of correlation cell with diameter ξ (termed as the correlation length) (see Fig. 1(a)). A correlation blob is composed of several stiff subunits which are assumed to be charged cylinders with radius a. Most of counterions are located in the electrical double layer (EDL) with thickness κ^{-1}. On the surface of the cylinder, electrical potential is ζ, whereas far away from the cylinder, $r \to \infty$, electrical potential is 0 (see Fig. 1(b)). Under alternating current (AC) electric field, some counterions with linear density ρ_l can move in the direction along axes of the EDL, which causes low-frequency (LF) relaxation. Some counterions with linear density ρ_h can move in the direction perpendicular to the axes of EDL, which causes LF relaxation.

The dielectric function $\varepsilon^*(\omega)$ includes LF and high-frequency (HF) relaxation terms:

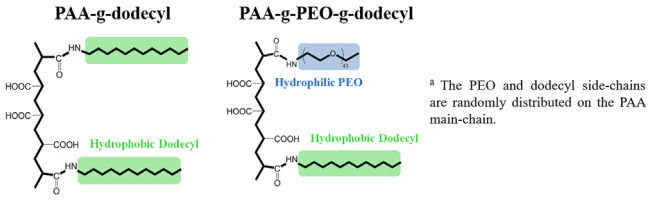

SCHEME 1 The illustration of structure of PAA-g-dodecyl and PAA-g-PEO-g-dodecyl Molecules. Note: The PEO and dodecyl side-chains are randomly distributed on the PAA main chain. [Color figure can be viewed at wileyonlinelibrary.com]

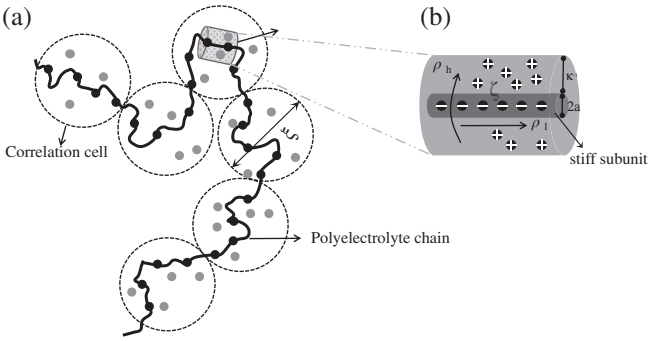

FIGURE 1 Schematic of DLPM of flexible PEs. (a) Chain configuration of a random walk of correlation cell with a diameter of ξ^3. (b) An EDL of a local stiff subunit, where ζ is the surface potential of the local stiff segment, ρ_l and ρ_h are the linear density of counterions fluctuating in the direction along and perpendicular to chains axes, respectively.

$$\varepsilon^*(\omega) = \varepsilon_l^*(\omega) + \varepsilon_h^*(\omega), \tag{1}$$

where $\varepsilon_h^*(\omega)$ is complex dielectric function of LF, $\varepsilon_h^*(\omega)$ is complex dielectric function of HF, and ω (=$2\pi f$, f is the measured frequency) is the angular frequency. The complex dielectric function of LF can be expressed as

$$\varepsilon_l^*(\omega) = \frac{\Delta\varepsilon_l}{1 + \left(\left(-i\omega\xi^2\right)/D_i\right)^{\alpha}}, \tag{2}$$

where ξ is the correlation length, D_i (= $k_B T M_i$) is the diffusivity of the counterions, M_i is the mobility of the counterions, α is distribution coefficient of LF relaxation. On the basis of the perturbation calculation of PE solution, the dielectric increment of LF relaxation can be defined as

$$\Delta\varepsilon_l = \frac{16\pi}{9}\frac{\varepsilon_s \varphi \xi}{\nu\kappa^2}\left(\frac{G_l}{G_0}\right)^2, \tag{3}$$

where ε_s is solvent permittivity, φ is the volume fraction of PE chains, ν is the monomer volume, κ^{-1} is the thickness of EDL around a stiff subunit. G_0(= $M_i q^2/l_B$) is the linear conductance of the counterions in the bulk, l_B is the distance at which the electrostatic interaction between two elementary charges in the medium is equal to the thermal energy $k_B T$, The contribution of counterions fluctuation along chains axis to linear conductance can be given as

$$G_l = M_i q \rho_l \tag{4}$$

The linear charged density of counterions that cause LF relaxation can be expressed as

$$\rho_l = -2\pi\varepsilon_0\varepsilon_s \frac{\kappa a K_1(\kappa a)}{K_0(\kappa a)}\zeta, \tag{5}$$

where ε_0 is vacuum dielectric constant, a is the radius of stiff subunit, ζ is the surface potential of the local stiff segment,

and K_α (α = 0.1) is the modified Bessel function, which is used to describe the distribution of electric potential around the charged cylinder.

The HF relaxation term can be expressed as

$$\varepsilon_h^*(\omega) = \frac{\Delta\varepsilon_h}{1 + (-i\omega/\omega_h)^\beta}, \quad (6)$$

where ω_h is the relaxation angular frequency and β is the distribution coefficient of HF relaxation. The dielectric increment of HF relaxation can be defined as

$$\Delta\varepsilon_h = \frac{2}{9\pi^2}\frac{\varphi G_h^2 \kappa}{\omega_h^2 \varepsilon_0^2 \varepsilon_s \nu}. \quad (7)$$

The contribution of counterions fluctuation perpendicular to chain axis to linear conductance can be given as

$$G_h = 2qM_i\rho_h\left(1 - \frac{1}{2\pi\eta l_B M_i}\right), \quad (8)$$

where η is the viscosity of the solvent. The linear charged density of counterions that cause HF relaxation can be given as

$$\rho_h = \frac{\pi\varepsilon_0\varepsilon_s\zeta^2}{4k_BT}\left(\frac{\kappa a K_1(\kappa a)}{K_0(\kappa a)}\right)^2 - \frac{\pi\varepsilon_0\varepsilon_s\zeta^2(\kappa a)^2}{4k_BT}. \quad (9)$$

EXPERIMENTAL SECTIONS

Materials and Preparation of the Samples

PAA-g-dodecyl and PAA-g-PEO-g-dodecyl (in Scheme 1) powders were prepared and purified by Prof. Charles C. Han's Research Group at the Institute of Chemistry, Chinese Academy of Sciences (Beijing, China). The method of preparing these polymers was described in Ref. [31]. According to the classical reaction of amino with carboxylic groups, different contents of PEO ($M_w \approx 2000$ g mol^{-1}) and dodecyl side chains were grafted onto the PAA ($M_w \approx 250{,}000$ g mol^{-1}) main chains. The molecular weights of PAA segment, PEO, and dodecyl segments were examined by ^{1}H NMR.[31] The molecular parameters of these copolymers are presented in Table 1.

DMF, which is partly polar because its dielectric constant ε is 36.7 F m^{-1}, and it dissolved solid samples of PAA-g-dodecyl and PAA-g-PEO-g-dodecyl. By adding double-distilled water (specific resistance was higher than 16 MΩ cm) into the mixture of grafted copolymer and DMF, sample solutions in DMF/H_2O solvent over the range of volume fraction of water, φ_{H_2O}, from 0 to 0.95 were prepared. In this case, the fraction of effective charges on PAA-g-dodecyl or PAA-g-PEO-g-dodecyl molecules, also called, is lower. Samples in solution with higher f_i were obtained by dripping 500 μL KOH solution at concentration of 0.5 M. pH values of samples at lower and high f_i were measured by pH meter (Mettler-Toledo, Delta 320). At φ_{H_2O} = 0, PH values are 6.3 and 8 for PAA-g-dodecyl samples, are 6.32 and 7.32 for PAA-g-PEO-g-dodecyl samples with low f_i and high f_i, respectively. At φ_{H_2O} = 0.95, pH values are 5.3 and 7.4 for PAA-g-dodecyl samples and 4.36 and 7.5 for PAA-g-PEO-g-dodecyl samples. The samples concentration is 2.5 mg ml^{-1}. The pH is just the measured value and used to distinguish between the samples with low f_i and high f_i at the same volume fraction of water. The samples concentration is 2.5 mg ml^{-1}.

Dielectric Measurements

Under an AC electric field, the dielectric response of a sample with angular frequency ω ($\omega = 2\pi f$, where f is the measurement frequency) is characterized by the complex permittivity $\varepsilon^*(\omega)$ as follows[32]:

$$\varepsilon^*(\omega) = \varepsilon'(\omega) - \frac{j\kappa(\omega)}{\omega\varepsilon_0} = \varepsilon(\omega) - j\left(\varepsilon''(\omega) + \frac{\kappa_l}{\omega\varepsilon_0}\right). \quad (10)$$

Here, $\varepsilon_0(\omega)$ is the real part of the complex permittivity (also called permittivity), $\varepsilon''(\omega)$ is the imaginary part of the complex permittivity (also called dielectric loss), $\kappa(\omega)$ is the frequency-dependent conductivity, and $j = (-1)^{1/2}$. In the polyelectrolyte solution, usually the total dielectric loss contains the effective dielectric loss of the sample and the direct current (DC) conductivity contribution. The contribution of DC conductivity κ_l can be subtracted from conductivity spectra by the equation $\varepsilon''(\omega) = (\kappa(\omega) - \kappa_l)/\varepsilon_0\omega$.[33–35] In this work, κ_l was read out from the platform of the conductivity spectra at several kHz. Then, dielectric loss data free of the DC conductivity effect was obtained. For the dielectric permittivity data, the eliminating of the electrode polarization (EP) was achieved by the fitting process with Cole–Cole equation containing the EP term $A\omega^{-m}$, then, parameters A and m of the EP term were determined.[34,35] Thus, a new $\varepsilon'(\omega)$ without the EP effect was derived by mathematically subtracting the $A\omega^{-m}$ from the raw permittivity. The dielectric loss spectra free of the DC conductivity effect were fitted by the Cole–Cole function. Fig. 2(a,b) are the representatives of dielectric loss spectra and fitting

TABLE 1 Characteristics of PAA-g-Dodecyl and PAA-g-PEO-g-Dodecyl Samples, Including Molecular Weight (M_w), the Molar Fraction of Side Chains (f_{PEO}, $f_{dodecyl}$) and the Weight Fraction of Side Chains (w_{PEO}, $w_{dodecyl}$)

	$M_w/10^5$	ω_{PEO} (wt %)	$\omega_{dodecyl}$ (wt %)	f_{PEO} (mol %)	$f_{dodecyl}$ (mol %)
PAA-g-dodecyl	3.4	–	26	–	13.4
PAA-g-PEO-g-dodecyl	3.3	7	19	0.27	10.5

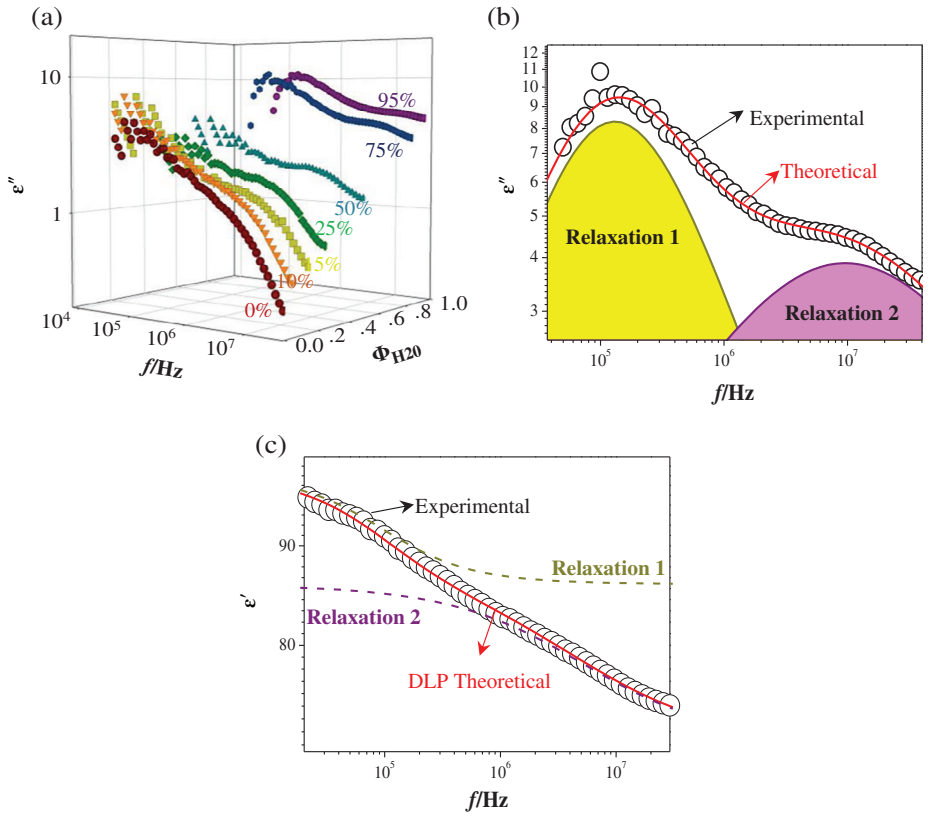

FIGURE 2 (a) The three-dimensional dielectric loss spectra of PAA-g-PEO-g-dodecyl molecules with low f_i in DMF/H_2O solvent after eliminating the effect of EP. (b) A representative result of the dielectric loss spectra after eliminating the effect of EP. (c) A representative fitting result of the dielectric spectra after eliminating the effect of EP. Black hollow circles represent the experimental permittivity data, and red solid lines represent the theoretical permittivity data calculated by DLP model using diffusivity of potassium ions $D = 0.77$ nm^2 s^{-1}.[36] Relaxations 1 and 2 are represented by solid dark yellow and purple dashed lines. [Color figure can be viewed at wileyonlinelibrary.com]

results. Remarkably, as seen from Fig. 2(a), two distinct peaks were found in the dielectric loss spectra. From Fig. 2(b), the contribution from Relaxation 1 in the area of light yellow (LF relaxation) and from Relaxation 2 in the area of light purple (HF relaxation) were obtained.

By combining eqs 1–4 and 6–8, the dielectric function $\varepsilon^*(\omega)$ in the framework of the DLP theory including two relaxation terms was obtained. By separating the real part and imaginary parts of the dielectric function $\varepsilon^*(\omega)$, we obtained the theoretical permittivity spectrum $\varepsilon'(\omega)$. Then, experimental permittivity spectra after eliminating the EP were fitted with the theoretical permittivity spectra of DLP model. The best curve fitting was guaranteed by the nonlinear least-squares method. Figure 2(c) shows a representative of the fitting results. Hollow circles represent experimental permittivity spectra after eliminating the effect of EP. Red line represents theoretical permittivity spectra of DLP model. The error analysis was discussed in the Supporting Information. It shows that the DLP theory is fairly accurate in fitting the experimental permittivity spectra. By means of the fitting, many valuable structural and electrical parameters of the samples including ξ, ρ_l, ρ_h, and κ^{-1} were obtained. Then, the ζ potential of a stiff subunit was calculated by substituting the parameters ρ_l, ρ_h, and κ^{-1} into eqs 5 and (9). The following discussion is based on these parameters.

RESULTS AND DISCUSSION

Conformational Transition of PAA-g-Dodecyl Molecules

In this study, the correlation length ξ, a key parameter described chains conformation of charged macromolecules in solution,[37] and ζ potential, which is widely used for quantification of the magnitude of net charges on chains and the degree of electrostatic repulsion between segments of a charged macromolecule,[38,39] were obtained by the fitting method described in Section 3.2. Figure 3(a) shows the dependence of correlation length of PAA-g-dodecyl molecules in DMF/H_2O solvent on φ_{H_2O}. Figure 3(b) shows the evolution of ζ potential (absolute value) for PAA-g-dodecyl at low and high f_i upon φ_{H_2O} increasing. Here, "High f_i" refers to the sample solutions at a series of water/DMF ratios which was added with the same amount of KOH solution. "low f_i" refers to the sample solutions which was not added with KOH solution. From Figure 3(a), with the increase of φ_{H_2O}, ξ increases in the range $0.1 < \varphi_{H_2O} < 0.3$ for PAA-g-dodecyl with lower fraction of effective charges f_i, and increases in the range $0.2 < \varphi_{H_2O} < 0.5$

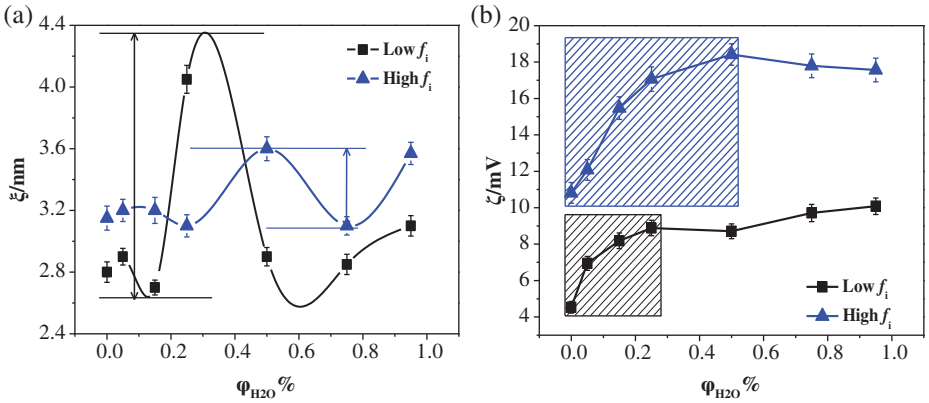

FIGURE 3 Correlation length (a) and ζ potential (b) of PAA-g-dodecyl molecules with low and high f_i in DMF/H_2O solvent as a function of φ_{H_2O}. [Color figure can be viewed at wileyonlinelibrary.com]

for that with higher f_i. From Figure 3(b), in the case of low f_i, the value of ζ potential increases with φ_{H_2O} below φ_{H_2O} = 0.3 (see shadow area with black color). In the case of high f_i, the value of ζ increases upon φ_{H_2O} increasing below φ_{H_2O} = 0.5 (see shadow area with blue color). It suggests the stretch of molecules in the range $0.1 < \varphi_{H_2O} < 0.3$ and $0.2 < \varphi_{H_2O} < 0.5$ for PAA-g-dodecyl at lower and higher f_i as seen from their increase of ξ in Figure 3(a), is due to the increase of electrostatic repulsion interaction between segments. As illustrated in Figure 4, over the lower φ_{H_2O} (Region I), as φ_{H_2O} increases, carboxylic acid groups gradually dissociate, so electrostatic repulsion interaction between segments increases. When it increases to a certain value, a stretched transition occurs.

In addition, as seen from Figure 3(a), with the increase of φ_{H_2O}, ξ abruptly decreases over the range $0.3 < \varphi_{H_2O} < 0.6$ for PAA-g-dodecyl at low f_i and over the range $0.5 < \varphi_{H_2O} < 0.75$ for that at high f_i. However, from Figure 3(b), ζ potential is basically invariable in the range $0.3 < \varphi_{H_2O} < 0.6$ and $0.5 < \varphi_{H_2O} < 0.75$ for PAA-g-dodecyl at low f_i and high f_i, respectively. It suggests that the decrease of ξ in Figure 3 (a) is not related to the change of electrostatic repulsion interaction between segments. It has been widely known that attractive interaction between hydrophobic groups increases with φ_{H_2O}.[3,40,41] Theoretically, Loh et al. obtained the relationship between the expansion factor α_e and the strength of excluded volume interaction for a uncharged hydrophobic polymer[12]:

$$\alpha_e^5 - \alpha_e^3 = \frac{4}{3}\left(\frac{3}{2\pi}\right)^{3/2} w\sqrt{N}, \quad (11)$$

Where α_e (= $R_g/R_{g,\theta}$, R_g is the gyration radius of a chain) is proportional to $\xi_g/\xi_{g,\theta}$,[42] w depends on the volume fraction of nonsolvent. It was showed that α_e remains unchanged and sharply decreases above a certain volume fraction of nonsolvent. Experimentally, they also observed an abrupt decrease of α_e. Based on the above work, the abruptly decrease of ξ for PAA-g-dodecyl at low and high f_i is predictable. As illustrated in Figure 4, over Region II, the attractive interaction among hydrophobic dodecyl groups plays an important role on chains conformation, as φ_{H_2OO} increases, the attractive interaction increases, so a collapsed transition occurs.

More interestingly, it can be seen from Figure 3(a) that the amount of ξ increasing and decreasing, or called increment and decrement, $\Delta\xi$, is closed for PAA-g-dodecyl molecules. It indicates that the electrostatic repulsion interaction between segments and attractive interaction among dodecyl groups are equally important in determining the conformational transition of PAA-g-dodecyl ($w_{dodecyl} \approx 26\%$) molecules in Regions I and II, respectively. Another phenomenon from Figure 3(a) is the value of $\Delta\xi$ is lower for PAA-g-dodecyl molecules with high f_i than those with low f_i (see black and blue arrows). It means that the transition of chain conformation with φ_{H_2O} is

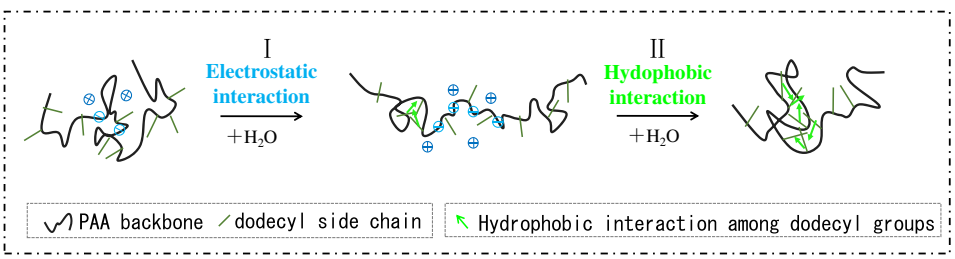

FIGURE 4 The schematic illustration of conformational transition of PAA-g-dodecyl molecules at low and high f_i with water content. [Color figure can be viewed at wileyonlinelibrary.com]

less pronounced for stronger charged chains. In general, electrostatic repulsion interaction between segments can be screened all or in part by counterions around chains, which is also considered as one of key factors to influence chains conformation.[43] According to the research by Essafi et al., the degree of intermolecular aggregation is higher for stronger charged hydrophobic polyelectrolytes.[14] It suggested that more counterions are distributed around a chain in the case of hydrophobic polyelectrolytes with high f_i. Thus, it can be predict that the screening degree of electrostatic repulsion interaction between segments is higher for PAA-g-dodecyl molecules with high f_i than those with low f_i. In this case, the stretching of chains conformation with increasing φ_{H_2O} is less pronounced for those with high f_i. In summary of above results, it confirms the roles of electrostatic repulsion interaction between segments and attractive interaction between hydrophobic groups in the evolution of chains conformation of PAA-g-dodecyl molecules and the possible influence of the fraction of effective charges on chains.

Conformational Transition of PAA-g-PEO-g-Dodecyl Molecules

Figure 5(a,c) shows the solvent dependence of correlation length ξ of PAA-g-PEO-g-dodecyl molecules ($w_{dodecyl} \approx 19\%$, $w_{PEO} \approx 7\%$) in the DMF/H_2O solvent obtained by DLPM dielectric analysis in Section 3.2. In the case of molecules with low f_i, ξ decreases below $\varphi_{H_2O} \approx 0.1$ and abruptly increases above $\varphi_{H_2O} \approx 0.75$ upon φ_{H_2O} increasing (see Fig. 5(a)). In the case of molecules with high f_i, ξ gradually increases from $\varphi_{H_2O} \approx 0.1$ to $\varphi_{H_2O} \approx 0.75$ (see Fig. 5(c)). Figure 5(b,d) shows the solvent dependence of ζ potential (absolute value) of PAA-g-PEO-g-dodecyl molecules in the DMF/H_2O solvent obtained by DLPM dielectric analysis in Section 3.2. At low f_i, the value of ζ decreases below $\varphi_{H_2O} \approx 0.1$ and there is also an abrupt increase above $\varphi_{H_2O} \approx 0.75$ upon φ_{H_2O} increasing (see Fig. 5 (b)). At high f_i, ζ potential gradually increases from $\varphi_{H_2O} \approx 0.1$ to $\varphi_{H_2O} \approx 0.75$ (see Fig. 5(d)). By comparison, from Fig. 5(a–d), the variation trends of ξ is basically consistent with the trends of ζ potential both for PAA-g-PEO-g-dodecyl molecules with low and high f_i (see shadow areas with green, purple and blue color). It indicates that their conformational transitions are mainly driven by electrostatic repulsion interaction between segments. As shown schematically in Fig. 6(a), with increasing φ_{H_2O}, PAA-g-PEO-g-dodecyl molecules with low f_i undergo an transition from an extended to a collapsed conformation due to the decrease of electrostatic repulsion interaction (Region I), and then undergo an abrupt transition from a collapsed to an extended conformation due to the increase of electrostatic repulsion interaction (Region II). As shown schematically in Fig. 6(b), at high f_i, molecules gradually stretch due to the increase of electrostatic repulsion interaction upon φ_{H_2O} increasing (Region I). Also, it can be concluded that the balance of electrostatic and hydrophobic interaction is influenced by the content of dodecyl groups. When the weight fraction of dodecyl groups is below 26%, the contribution of electrostatic interaction to chains conformation is greater than hydrophobic interaction (see the schematic illustration in Fig. 7).

Even so, the role of attractive interaction among hydrophobic dodecyl groups on their conformation cannot be totally ignored because it may influence electrostatic repulsion interaction and thus affect chains conformation. From Figure 5(b, d), there is a slight decrease in ζ potential below $\varphi_{H_2O} \approx 0.1$ both for PAA-g-PEO-g-dodecyl at low and high f_i. The result implies that small amount of counterions condense onto chains when H_2O is added to PAA-g-PEO-g-dodecyl/DMF solution. Up to now, extensive research studies have revealed that some counterions easily condense into hydrophobic microdomain where dielectric constant is very low for polyelectrolyte containing hydrophobic groups,[4,43,44] So it cannot be excluded that the condensation of counterions is due to the formation of hydrophobic dodecyl microdomain when H_2O is added to PAA-g-PEO-g-dodecyl/DMF solution. As schematically illustrated in

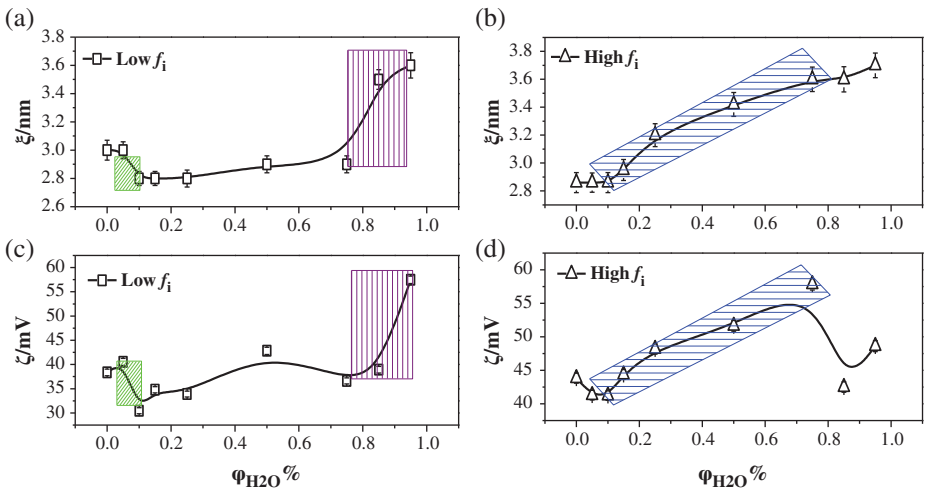

FIGURE 5 Correlation length (a,c) and ζ potential (b,d) of PAA-g-PEO-g-dodecyl molecules with low and high f_i in DMF/H_2O solvent as a function of φ_{H_2O}. [Color figure can be viewed at wileyonlinelibrary.com]

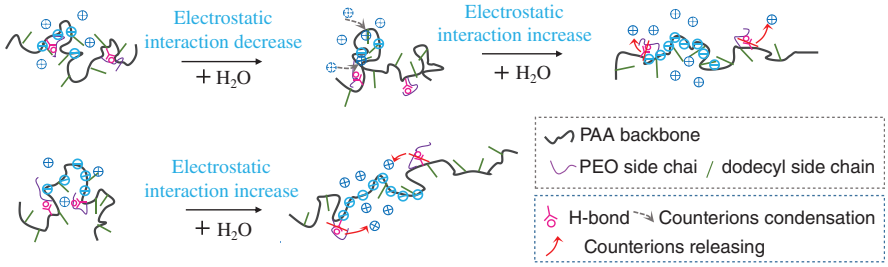

FIGURE 6 The schematic illustration of conformational transition of PAA-g-PEO-g-dodecyl molecules (a) at low and (b) high f_i in DMF/H_2O solvent with water content. [Color figure can be viewed at wileyonlinelibrary.com]

Figure 6, below $\varphi_{H_2O} \approx 0.1$ (in Region I), upon φ_{H_2O} increasing, small amount of counterions condense into microdomain containing dodecyl groups and result in the decrease of ξ in Figure 5a for PAA-g-PEO-g-dodecyl at low f_i.

In addition, from Figures 3b and 5b, it should be noted that ζ potential increases from $\varphi_{H_2O} \approx 0$ to $\varphi_{H_2O} \approx 0.3$ for PAA-g-dodecyl; however, ζ potential increases from $\varphi_{H_2O} \approx 0.75$ to $\varphi_{H_2O} \approx 0.95$ for PAA-g-PEO-g-dodecyl at low f_i. From Figures 3b and 5d, ζ potential increases from $\varphi_{H_2O} \approx 0$ to $\varphi_{H_2O} \approx 0.5$ for PAA-g-dodecyl; however, ζ potential increases from $\varphi_{H_2O} \approx 0.1$ to $\varphi_{H_2O} \approx 0.75$. By comparison, the increase of ζ potential for PAA-g-PEO-g-dodecyl occurs over the higher φ_{H_2O} range than PAA-g-dodecyl. A possible reason is grafting PEO side chains, which can introduce many intramolecular or intermolecular hydrogen bonds (also called H-bonds) between C—O from alkoxy groups and O—H from carboxyl groups.[31] In fact, the formation of H-bond between the carboxyl proton of PAA and the ether oxygen of PEO in the solution or solid state has been extensively confirmed by some experimental technologies, directly, including nuclear magnetic resonance spectra[45,46] and electron spin resonance spin probe,[47] infrared spectroscopy,[48] indirectly, including turbidity measurement,[49] light scattering light scattering.[27,50] The results showed that in H_2O/DMF mixed solvent, the number of H-bond between the carboxyl proton and the ether oxygen increases as φ_{H_2O} increases.[45,50,51] Considering the formation of H-bonds, it is not difficult to explain above results. As illustrated in Figure 6, the formation of H-bonds will prevent the dissociation of free carboxyl groups at lower φ_{H_2O},[28] thus the increase of ζ potential for PAA-g-PEO-g-dodecyl moves to higher φ_{H_2O}(see the pink marks and red arrows).

In the end, a phenomenon that caught our attention is the decrease of ζ potential above $\varphi_{H_2O} \approx 0.7$ for PAA-g-PEO-g-dodecyl molecules at high f_i in Figure 5(d). The dramatic decrease of ζ potential suggests that a strong counterions condensation occurs. We think there are two possibilities of the strong condensation. One is the condensation of counterions into hydrophobic microdomain containing dodecyl groups which has been found in hydrophobic polyelectrolyte.[4,43,44] If this type of condensation occurs, chains will tend to collapse.[4,43,44] The other possibility is the effect of counterions bridging between "adjacent" charged monomers, leading to a more locally stretched conformation.[52] H-bond between C—O from alkoxy groups and O—H from carboxyl groups will enhance the local bridging behavior associated with the

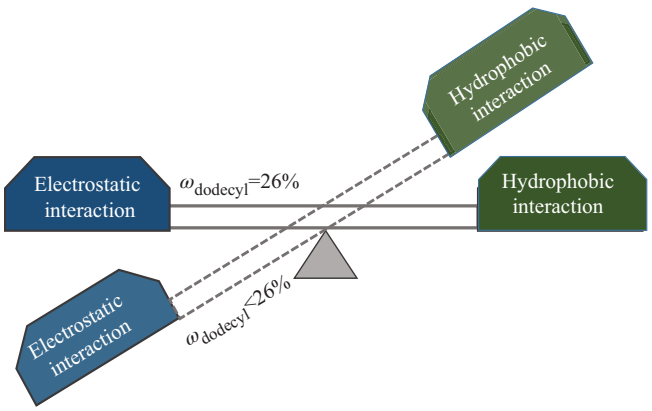

FIGURE 7 A schematic illustration of the influence of the content of dodecyl groups on the balance of electrostatic and attractive interactions in determining conformational transition. [Color figure can be viewed at wileyonlinelibrary.com]

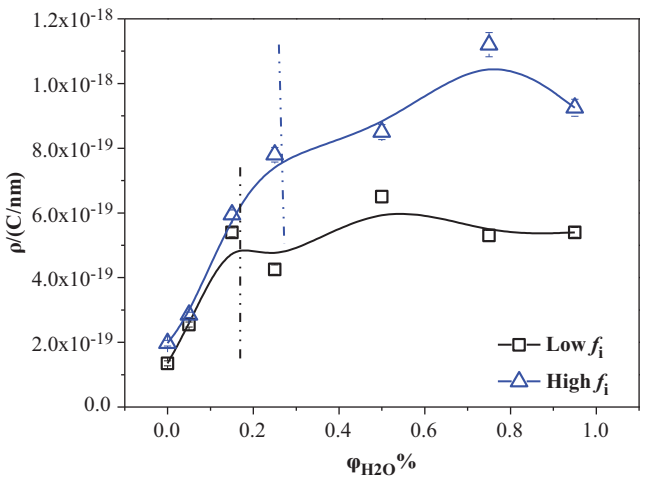

FIGURE 8 Linear density of counterions around a chain for PAA-g-dodecyl molecules with low and high f_i in DMF/H_2O solvent as a function of φ_{H_2O}. [Color figure can be viewed at wileyonlinelibrary.com]

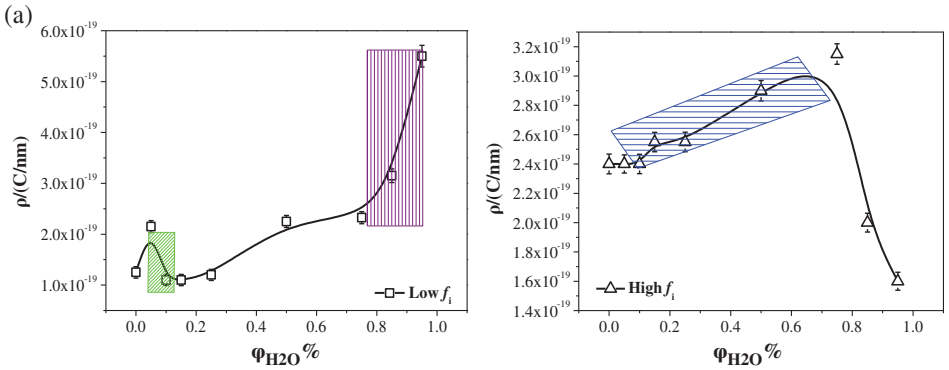

FIGURE 9 Linear density of counterions around a chain for PAA-g-PEO-g-dodecyl molecules with (a) low and (b) high f_i in DMF/H_2O solvent as a function of φ_{H_2O}. [Color figure can be viewed at wileyonlinelibrary.com]

counterions condensation.[53] In this case, a strong condensation occurs without chain collapsing.[53] From Figure 5(c), there is no decrease of ξ above $\varphi_{H_2O} \approx 0.7$. Thus, compared to the former prediction, the latter seems to be more appropriated to explain the decrease of ζ potential in Figure 5(d).

Role of Counterions Distribution on Conformational Transition

The linear density of counterions around a chain for PAA-g-dodecyl and PAA-g-PEO-g-dodecyl molecules ($\rho = \rho_l + \rho_h$) is obtained by dielectric analysis with DLPM as described in Section 3.2. Figure 8 shows the dependence of linear density of counterions around chains on φ_{H_2O} for PAA-g-dodecyl molecules in DMF/H_2O solvent. ρ for PAA-g-dodecyl with low f_i and high f_i increase below $\varphi_{H_2O} \approx 0.15$ and below $\varphi_{H_2O} \approx 0.25$ upon φ_{H_2O} increasing, respectively, which leads to an increase of the shielding effect of electrostatic repulsion interaction between segments. It is one of the possible reasons that ξ of PAA-g-dodecyl with low and high f_i is invariable below $\varphi_{H_2O} \approx 0.2$ and $\varphi_{H_2O} \approx 0.3$ as shown in Figure 3(a), respectively.

Figure 9 shows the dependence of linear density of counterions around a chain on φ_{H_2O} for PAA-g-PEO-g-dodecyl molecules in DMF/H_2O solvent. As seen from Figure 9(a), there are an abrupt increase above $\varphi_{H_2O} \approx 0.75$ and a slight decrease around $\varphi_{H_2O} \approx 0.05$ for PAA-g-PEO-g-dodecyl with low f_i (see purple and green shadows). The trend is similar to the φ_{H_2O} dependency of ζ potential in Figure 5(b) (see purple and green shadows). As seen from Figure 9b, ρ increases from $\varphi_{H_2O} \approx 0.1$ to $\varphi_{H_2O} \approx 0.75$ (see blue shadow). An increase of ζ potential is also found from $\varphi_{H_2O} \approx 0.1$ to $\varphi_{H_2O} \approx 0.75$ in Figure 5(d) (see blue shadow). It is easy to understand because the counterions distribution is directly related to the numbers of counterions around a chain. In addition, ρ decreases above $\varphi_{H_2O} \approx 0.75$ for PAA-g-PEO-g-dodecyl molecules with high f_i as seen from Figure 9(b), which causes a decrease of shielding effect of electrostatic repulsion interaction between segments. Therefore, ξ for them fails to decrease above $\varphi_{H_2O} \approx 0.75$ (see Fig. 5(c)), although the value of ζ potential decreases (see Fig. 5(d)).

CONCLUSIONS

In summary, by using double-layer polarization theory to analyze the dielectric data measured in this work, several microstructural and electrical parameters were obtained, from which the roles of electrostatic and hydrophobic interactions in determining conformational transition are revealed for PAA-g-dodecyl and PAA-g-PEO-g-dodecyl molecules in DMF/H_2O mixed solvent. In case of PAA-g-dodecyl molecules, in addition to the collapsed transition with the increase of water content resulting from the increase of hydrophobic interaction, we also found a transition from collapsed to stretched structure. We learned that the transition is originated from the increase of electrostatic interaction with water content. For PAA-g-PEO-g-dodecyl molecules, at low fraction of effective charges, they undergo a transition from stretched to collapsed and then to stretched structure, at high fraction of effective charges, they undergo a transition from collapsed to stretched structure. We learned that their conformational transition is originated from the change of electrostatic interaction.

Furthermore, it is revealed that the balance of electrostatic and attractive interaction in determining conformational transition of PAA-g-dodecyl groups is influenced by the content of dodecyl groups. When the weight fraction of dodecyl groups is about 26%, electrostatic and attractive repulsion interactions are equally important. When the weight fraction of dodecyl groups is below 26%, the contribution of attractive repulsion interaction among dodecyl groups can be ignored. In addition, our insight into the roles of PEO side chains on the evolution of electrostatic interaction of PAA-g-dodecyl molecules was given. The formation of H-bonds between alkoxy groups of PEO side chains and carboxylic acid groups of PAA backbone will prevent the dissociation of free carboxyl groups over the range of low φ_{H_2O}, thus the increase of electrostatic repulsion interaction between segments moves to higher φ_{H_2O} for PAA-g-PEO-g-dodecyl. Besides, the results of

linear density of counterions suggest that the distribution of counterions may influence their conformational transition. This overall work opens opportunities for understanding the balance of various interactions in the process of solvent-induced transition of chains conformation of polyelectrolytes with hydrophobic groups.

ACKNOWLEDGMENTS

The authors gratefully thank Dr Jin-kun Hao (The Institute of Chemistry, The Chinese Academy of Science, China) for supplying the sample used in this experiment. This work was financially supported by the National Natural Science Foundation of China (Nos. 21673002, 21473012).

REFERENCES

1 D. Hinderberger, G. Jeschke, H. W. Spiess, *Macromolecules* **2002**, *35*, 9698.

2 S. Förster, M. Schmidt, *Phys. Prop. Polym.* **1995**, *120*, 51.

3 A. V. Dobrynin, M. Rubinstein, *Macromolecules* **1999**, *32*, 915.

4 A. V. Dobrynin, M. Rubinstein, *Macromolecules* **2001**, *34*, 1964.

5 H. Tang, Q. Liao, P. Zhang, *J. Chem. Phys.* **2014**, *140*, 194905.

6 A. V. Lyulin, B. Dünweg, O. V. Borisov, A. A. Darinskii, *Macromolecules* **1999**, *32*(10), 3264.

7 W. Essafi, M. N. Spiteri, C. Williams, F. Boué, *Macromolecules* **2009**, *42*, 9568.

8 S. S. Muralidharan, U. Natarajan, *Mol. Simulat.* **2013**, *39*, 145.

9 S. Praveenkumar, N. Upendra, *J. Mol. Graph. Model.* **2016**, *64*, 60.

10 M. Boas, G. Vasilyev, R. Vilensky, Y. Cohen, E. Zussman, *Polymers* **2019**, *11*(6), 1053.

11 M. Boas, A. Gradys, G. Vasilyev, M. Burman, E. Zussman, *Soft Matter* **2015**, *11*, 1739.

12 P. Loh, G. R. Deen, D. Vollmer, K. Fischer, *Macromolecules* **2008**, *41*, 9352.

13 A. Kiriy, G. Gorodyska, S. Minko, W. Jaeger, *J. Am. Chem. Soc.* **2002**, *124*, 13454.

14 W. Essafi, A. Abdelli, G. Bouajila, *J. Phys. Chem. B.* **2012**, *116*, 13525.

15 D. Ghosh, A. Bhattarai, B. Das, *Colloid Polym. Sci.* **2009**, *287*, 1005.

16 V. O. Aseyev, S. I. Klenin, H. Tenhu, *J Polym Sci B* **1998**, *36*, 1107.

17 Y. F. Wei, P. Y. Hsiao, *J. Chem. Phys.* **2010**, *132*, 024905.

18 S. Liu, M. Muthukumar, *J. Chem. Phys.* **2002**, *116*, 9975.

19 M. A. Winnik, A. Yekta, *Curr. Opin. Colloid Interface Sci.* **1997**, *2*(4), 424.

20 J. Koetz, S. Kosmella, T. Beitz, *Prog. Polym. Sci.* **2001**, *26*, 1199.

21 Z. Iatridi, V. Georgiadou, M. Menelaou, *Dalton Trans.* **2014**, *43*, 8633.

22 F. Bordi, C. Cametti, G. Paradoss, *J. Phys. Chem.* **1992**, *96*, 8194.

23 L. CYD, *Phys. Rev. E* **2011**, *84*, 041804.

24 D. Truzzolillo, C. Cametti, S. Sennatoab, *Phys. Chem. Chem. Phys.* **2009**, *11*, 1780.

25 M. Luksic, R. Buchner, B. Hribar-Lee, V. Vlachy, *Macromolecules* **2009**, *42*(12), 4337.

26 T. Mitsumata, T. Miura, N. Takahashi, M. Kawai, *Phys. Rev. E* **2013**, *87*, 042607.

27 Z. Chen, X. W. Li, K. S. Zhao, *J. Phys. Chem.* **2011**, *115*(19), 5766.

28 X. L. Zhou, K. S. Zhao, *Phys. Chem. Chem. Phys.* **2017**, *19*, 20559.

29 X. L. Zhou, K. S. Zhao, *Soft Matter.* **2018**, *14*, 1130.

30 X. L. Zhou, K. S. Zhao, *Soft Matter* **2018**, *14*(35), 7190.

31 J. K. Hao, Z. Y. Li, H. Cheng, C. Wu, C. C. Han, *Macromolecules* **2010**, *43*, 9534.

32 H. Schwan, *Determination of Biological Impedances, Physical Techniques in Biological Research*; Academic Press, Inc: New York, NY, **1963**.

33 F. Bordi, *Bioelectrochemistry* **2001**, *54*, 53.

34 J. L. Li, K. S. Zhao, *Phys. Chem. Chem. Phys.* **2015**, *17*, 4175.

35 J. L. Li, K. S. Zhao, *J. Phys. Chem. B* **2013**, *117*, 11843.

36 H. S. Harned, R. L. Nuttall, *J. Am. Chem. Soc.* **1949**, *71*, 1460.

37 A. V. Dobrynin, R. H. Colby, M. Rubinstein, *Macromolecules* **1995**, *28*, 1859.

38 J. A. Schellman, *Biopolymers* **1977**, *16*, 1415.

39 B. J. Kirby, E. F. Hasselbrink Jr., *Electrophoresis* **2004**, *25*, 203.

40 H. H. Hooper, S. Beltran, A. P. Sassi, H. W. Blanch, J. M. Prausnitz, *J. Chem. Phys.* **1990**, *93*, 2715.

41 M. D. Carbajal-Tinoco, R. Ober, I. Dolbnya, W. Bras, C. E. Williams, *J. Phys. Chem. B* **2002**, *106*, 12165.

42 J. R. C. Van der Maarel, *Introduction to Biopolymer Physics*; World Scientific: Singapore, **2008**, p. 264.

43 A. V. Dobrynin, M. Rubinstein, *Prog. Polym. Sci.* **2005**, *30*, 1049.

44 W. Essafi, F. Lafuma, D. Baigl, C. E. Williams, *Europhys. Lett.* **2005**, *71*(6), 938.

45 O. Hiroyuki, A. Koji, T. Eishun, *Macromol. Chem. Phys.* **1978**, *179*, 755.

46 M. Toshikazu, K. Takegoshi, H. Kunio, *Polymer* **1997**, *38*(10), 2315.

47 T. Li, S. M. Chen, Z. Chen, Y. M. Shen, *Magn. Reson. Chem.* **2003**, *41*, 481.

48 N.-D. Sergio, P. Jorge, K. Issa, *Macromol. Chem. Phys.* **2001**, *202*, 3106.

49 Y. Cohen, V. Prevysh, *Acta Polym.* **1998**, *49*, 539.

50 M. L. Xiang, M. Jiang, Y. B. Zhang, W. C. Feng, *Macromolecules* **1997**, *30*, 2313.

51 V. Khutoryanskiy, *Hydrogen-Bonded Interpolymer Complexes: Formation, Structure and Applications*; World Scientific: Singapore, **2009**.

52 Y.-T. Chung, C.-I. Huang, *J. Chem. Phys.* **2012**, *136*, 124903.

53 S. P. Ju, W. J. Lee, C. I. Huang, W. Z. Cheng, Y. T. Chung, *J. Chem. Phys.* **2007**, *126*, 224901.